Three-dimensional effects on cracked discs and plates under nominal Mode III loading

A. Campagnolo, F. Berto
University of Padova, Department of Management and Engineering, Stradella S. Nicola 3, 36100, Vicenza (Italy)
campagnolo@gest.unipd.it, berto@gest.unipd.it

L. P. Pook
21 Woodside Road, Sevenoaks TN13 3HF (United Kingdom)
les.pook@tesco.net

ABSTRACT. The existence of three-dimensional effects at cracks has been known for many years, but understanding has been limited, and for some situations still is. Understanding improved when the existence of corner point singularities and their implications became known. Increasingly powerful computers made it possible to investigate three-dimensional effects numerically in detail. Despite increased understanding, three-dimensional effects are sometimes ignored in situations where they may be important. The purpose of the present contribution is to review the study carried out by the same authors in some recent investigations, in which a coupled fracture mode generated by anti-plane loading of a straight through-the-thickness crack in linear elastic discs and plates has been analysed by means of accurate 3D finite element (FE) models.
The results obtained from the highly accurate finite element analyses have improved understanding of the behaviour of through cracked components under anti-plane loading. The influence of plate bending is increasingly important as the thickness decreases. It appears that a new field parameter, probably a singularity, is needed to describe the stresses at the free surfaces. Discussion on whether K_{III} tends to zero or infinity as a corner point is approached is futile because K_{III} is meaningless at a corner point.
The intensity of the local stress and strain state through the thickness of the cracked components has been evaluated by using the strain energy density (SED) averaged over a control volume embracing the crack tip. The SED has been considered as a parameter able to control fracture in some previous contributions and can easily take into account also coupled three-dimensional effects. Calculation of the SED shows that the position of the maximum SED in the discs case is a function of the thickness. In the plates case instead the position of the maximum SED is independent of plate thickness, contrary to disc results.

KEYWORDS. Fracture mechanics; Finite element analysis; Anti-plane loading; Stress intensity factor; Corner point effects.

INTRODUCTION

Crack tip surface displacements in the vicinity of a corner point in which a crack front intersects a surface are often of practical interest. Assuming that Poisson's ratio, $\nu > 0$, then kinematics considerations for an antisymmetric loading [1] show that modes II and III crack tip surface displacements cannot exist in isolation. Mode II induces

mode III^c and mode III induces mode II^c. These induced modes are sometimes called coupled modes, indicated by the superscript c.

The existence of three-dimensional effects at cracks has been known for many years [2-4], but understanding has been limited, and for some situations still is. Understanding improved when the existence of corner point singularities [5] and their implications became known [6]. Despite increased understanding, three-dimensional effects are sometimes ignored in situations where they may be important.

Within the framework of linear elastic fracture mechanics [7] the stress field in the vicinity of a crack tip is dominated by the leading term of a series expansion of the stress field [8]. This leading term is the stress intensity factor, K. In three dimensional geometries, the derivation of stress intensity factors makes the implicit assumption that a crack front is continuous. This is not the case in the vicinity of a corner point, and the nature of the crack tip singularity changes. The resulting corner point singularities were described in detail in 1979 by Bažant and Estenssoro [5]. Some additional results were given by Benthem in 1980 [9]. For corner point singularities, the polar coordinates are replaced by spherical coordinates (r, θ, ϕ) with origin at the corner point. The angle ϕ is measured from the crack front.

There do not appear to be any exact analytic solutions for corner point singularities. In their analysis Bažant and Estenssoro [5] assumed that all three modes of crack tip surface displacement are of the form $r^{\lambda}\varrho^{p}F(\theta, \phi)$, where ϱ is distance from the crack tip, and p is a given constant. They then calculated λ numerically for a range of situations: λ is a function of Poisson's ratio, υ. For the antisymmetric mode, $\lambda = 0.598$ for $\upsilon = 0.3$. Benthem [9] made an equivalent assumption but used a different numerical method to calculate λ. The stress intensity measure, K_{λ}, may be used to characterise corner point singularities, where λ can be regarded as a parameter defining the corner point singularity. However, expressions for numerical values of K_{λ}, and associated stress and displacement fields, do not appear to be available. At the present state of the art the extent of a corner point singularity dominated region has to be determined numerically.

At a corner point stresses are a singularity. They must be either infinite or zero, λ is indeterminate, and it is reasonable to speak of stress intensity factors in an asymptotic sense [2,3]. In the limit, as a crack front is approached, displacement fields must be those of a stress intensity factor [9]. Hence, there is an infinitesimal K-dominated region within the core region of a corner point singularity. The stress intensity factors are proportional to $s^{0.5 - \lambda}$ where s is the distance from the surface along the z axis [9]. Hence, for the antisymmetric mode K_{II} and K_{III} both tend to infinity as a corner point is approached. Further, as a corner point the ratio K_{III}/K_{II} tends to a limiting value which is a function of υ. For $\upsilon = 0.3$ the limiting ratio is 0.5 [9]. Benthem points out that K_{II} and K_{III} lose their meaning at a corner point [9]. Dhondt suggests that modes II^c and III^c might not be singular [10]. The predicted tendency to infinity is reasonable for K_{II} since relevant stresses are in plane and disclinations are zero [2,3]. From a linear elastic viewpoint the predicted tendency of K_{III} to infinity cannot be correct [4]. At a surface shear stresses perpendicular to the surface are zero, which implies that K_{III} tends to zero as the surface is approached. Mode III is a torsion problem [11]. Under mode III (anti-plane) loading initially plane cross sections, including the surface at a corner point, do not remain plane under load [4] and disclinations appear. It is well known that serious error can arise if warping of non-circular cross sections under torsion is not taken into account in stress analyses [12]. Warping of the surface under mode III means that τ_{yz} at the surface does not have to be zero, and finite values of K_{III} are possible. The implication is that the non linearities cannot be regarded as being in a core region within a corner point singularity dominated region and that Bažant and Estenssoro's prediction that K_{III} tends to infinity as a corner point is correct. The alternative view, which is supported by a large body of evidence [4], is that apparent values of K_{III} decrease towards the surface in the z direction. This implies that K_{III} tends to zero as a corner point is approached, which is intuitively correct. It also implies that non linearities can be regarded as being within a core region, but does not explain why Bažant and Estenssoro's analysis does not give the correct limit. Nevertheless, this alternative view may well be adequate when considering practical implications. This paradox needs to be resolved so that the results of finite element analysis can be interpreted correctly.

There does not appear to have been a systematic investigation of the extent to which Bažant and Estenssoro's initial assumption is justified. Their assumption does appear to be satisfactory for the symmetric mode (mode I) in that their analysis leads to useful results [4]. The purpose of the present contribution is to review the study carried out by the same authors in some recent investigations [2,3], in which a coupled fracture mode generated by anti-plane loading of a straight through-the-thickness crack in linear elastic discs and plates has been analysed by means of accurate 3D finite element (FE) models.

Due to the uncertainties in the definition of the stress intensity factors on the free surfaces, as stated above, the strain energy density averaged in a control volume (SED) has been employed to quantify the stress intensity through the thickness of the discs [2] and plates [3]. For a review of the SED the reader can refer to [13]. This parameter has been successfully used by Lazzarin and co-authors to assess the fracture strength of a large bulk of materials, characterized by

different control volumes, subjected to wide combinations of static loading [14 - 16] and the fatigue strength of notched components [17, 18]. As described in [13, 19] an intrinsic advantage of the SED approach is that it permits automatically to take into account higher order terms and three-dimensional effects. The parameter is easy to calculate in comparison with other well-defined and suitable 3D parameters [20, 21] and can be directly obtained by using coarse meshes [13, 19]. Another advantage of the SED is that it is possible to easily understand whether the through-the-thickness effects are important or not in the fracture assessment for a specific material characterized by a control volume depending on the material properties. Some brittle materials are characterized by very small values of the control radius and are very sensitive to stress gradients also in a small volume of material [13]. On the other hand more ductile materials have the capability of stress averaging in a larger volume and for this reason are less sensitive to the variations of the stress field through the thickness of the component. The SED, once the control volume is properly modeled through the thickness of the disc or plate, is able to quantify the 3D effects in comparison with the sensitivity of the specific material so providing precious information for the fracture assessment.

FINITE ELEMENT MODELLING

STresses and stress intensity factors have been examined in detail for 100 mm diameter discs [2] and 100 mm square plates [3] of various thicknesses under anti-plane (nominal mode III) loading. The thickness is t for both components while in the discs case the radius, r, is 50 mm. A through thickness crack has its tip at the centre of the component, so its length, a, is 50 mm. Calculations have been carried out using ANSYS 11 for t/a = 0.25, 0.5, 0.75, 1, 1.25, 1.5, 1.75, 2, 2.25, 2.5, 2.75 and 3. Poisson's ratio is taken as 0.3 and Young's modulus as 200 GPa. In the discs case, displacements corresponding to K_{III} = 1 MPa·m$^{0.5}$ (31.62 N·mm$^{0.5}$) have been applied to the cylindrical surface, while in the plates case a displacement of 10^{-3} mm has been applied to the edge of the plate. Stress intensity factors have been calculated from stresses on the crack surface near the crack tip using standard equations [7,11]. The strain energy density has been calculated from a control volume at the crack tip. One quarter of the cracked component has been modelled. An overall view of the finite element meshes is shown in Fig. 1a for the discs case and in Fig. 1b for the plates one.

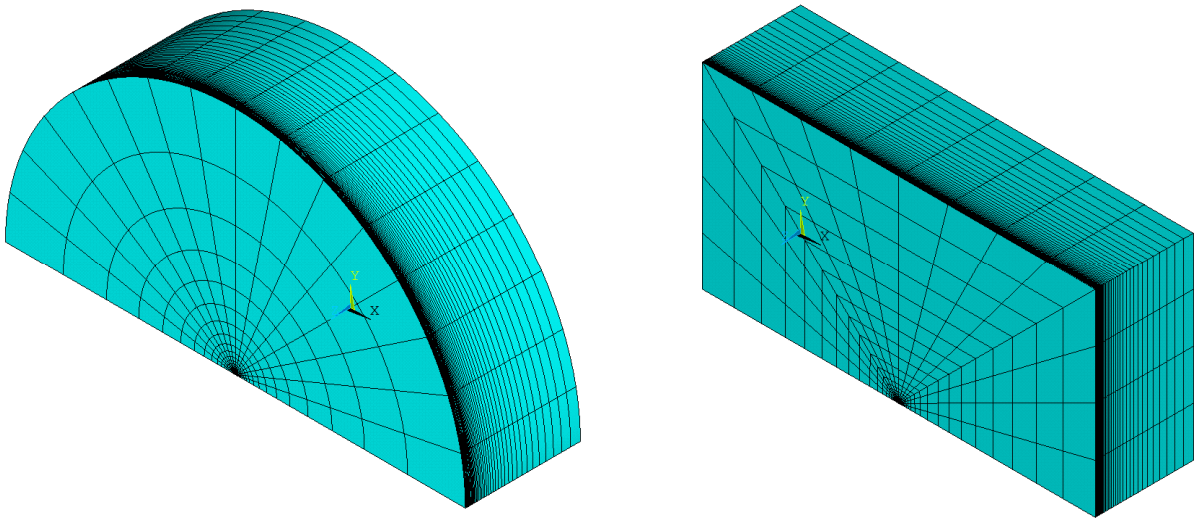

Figure 1: Overall view of finite element meshes. (a) disc and (b) plate.

RESULTS

Crack surface stresses, τ_{yz} and τ_{xy} have been extracted from the finite element results at distances, s, from the disc and plate surfaces of 0 mm, 0.25 mm and 1 mm. Results for t/a = 1 and s = 0 mm and 1 mm, plotted on logarithmic scales, are shown in Figs. 2-3 with reference only to discs case for the sake of brevity. Results for other values of t/a and with reference to plates case are generally similar, but with some differences in detail. When the plot is a straight line its slope is -λ. Values of λ taken from straight line plots, related to both discs and plates, are shown in Tabs.1 and 2. Where no value is shown the plot could not be regarded as a straight line.

For $s \geq 0.25$ mm the value of λ calculated from τ_{xy} is close to the theoretical value of 0.5 for a stress intensity factor singularity (Tab. 1). Hence, realistic values of K_{II} can be calculated. For $s = 0$ mm, in the discs case λ increases as t/a increases, this is in contrast to the plate results where the value of λ has a maximum for $t/a = 0.25$, and decreases as t/a increases. The values of λ are all significantly less than the theoretical value of 0.598 for a corner point singularity. Realistic values of K_{II} can probably be calculated for $t/a \geq 0.25$ mm. Realistic values of K_{III} can be calculated from τ_{yz} for $s \geq 1$ mm. The results for $s = 0$ mm (Fig. 2) show that τ_{yz} is slightly lower than τ_{xy} for small x, and decreases as x increases. Realistic values of K_{III} cannot be calculated. The presence of finite values of τ_{yz}, linked to finite values of K_{III} (Fig. 4), appears because of the appearance of mode I disclinations, which are rotations about the y axis. Differentiating the expression for the displacement U_z gives the amount of this rotation which increases towards the crack tip, with a concomitant increase in τ_{yz} at a surface. This accounts qualitatively for the observed distributions of τ_{yz} at a surface.

t/a	$s = 0$ mm		$s = 0.25$ mm		$s = 1$ mm	
	disc	plate	disc	plate	disc	plate
0.25	0.505	0.538	0.497	0.498	0.497	0.497
0.50	0.520	0.527	0.497	0.498	0.497	0.497
0.75	0.530	0.523	0.497	0.498	0.497	0.497
1.00	0.538	0.520	0.497	0.498	0.497	0.497
1.25	0.544	0.517	0.497	0.498	0.497	0.497
1.50	0.549	0.515	0.497	0.498	0.497	0.497
1.75	0.553	0.513	0.497	0.498	0.497	0.497
2.00	0.556	0.512	0.497	0.498	0.497	0.497
2.25	0.559	0.510	0.497	0.498	0.497	0.497
2.50	0.542	0.510	0.497	0.498	0.497	0.497
2.75	0.545	0.509	0.497	0.498	0.497	0.497
3.00	0.547	0.508	0.497	0.498	0.497	0.497

Table 1: Values of λ for τ_{xy}, s is the distance from the surface in the z direction.

t/a	$s = 0$ mm		$s = 0.25$ mm		$s = 1$ mm	
	disc	plate	disc	plate	disc	plate
0.25	-	-	-	-	0.508	0.507
0.5	-	-	-	-	0.506	0.506
0.75	-	-	-	-	0.507	0.506
1.00	-	-	-	-	0.507	0.506
1.25	-	-	-	-	0.506	0.506
1.50	-	-	-	-	0.506	0.506
1.75	-	-	-	-	0.506	0.506
2.00	-	-	-	-	0.506	0.506
2.25	-	-	-	-	0.507	0.506
2.50	-	-	-	-	0.506	0.505
2.75	-	-	-	-	0.506	0.506
3.00	-	-	-	-	0.507	0.506

Table 2: Values of λ for τ_{yz}, s is the distance from the surface in the z direction.

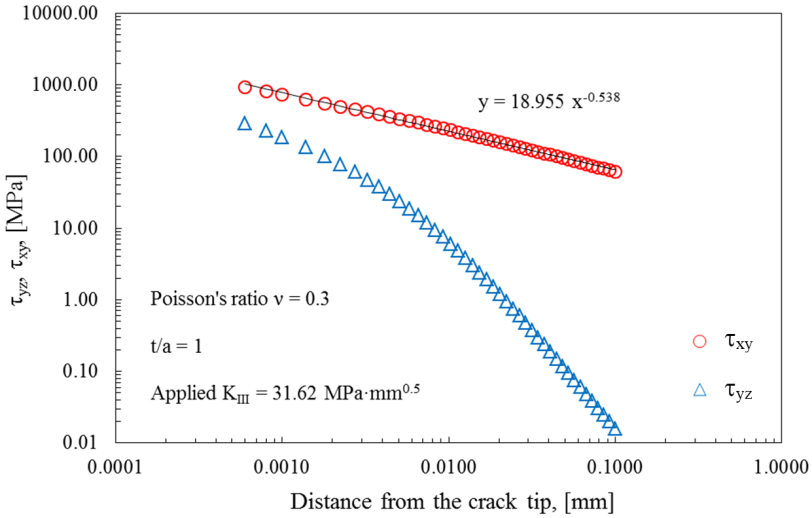

Figure 2: Discs case: stresses τ_{yz} and τ_{xy} on crack surface at s = 0 mm from disc surface, t/a =1.

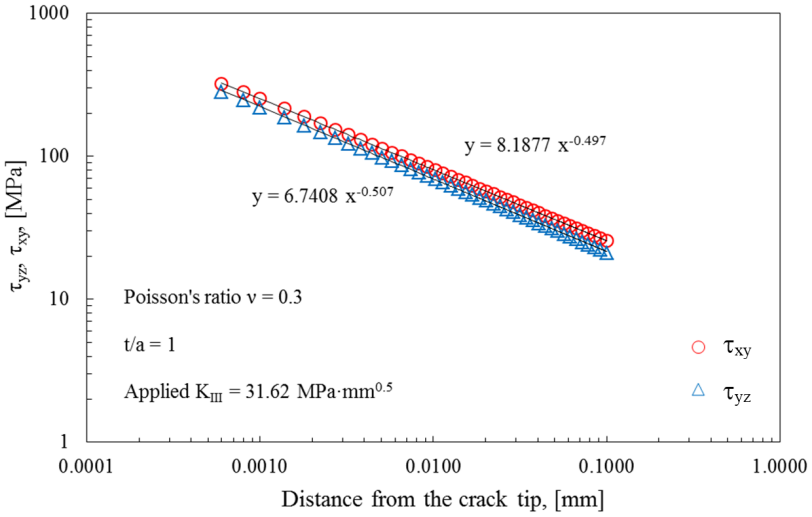

Figure 3: Discs case: stresses τ_{yz} and τ_{xy} on crack surface at s = 1 mm from disc surface, t/a =1.

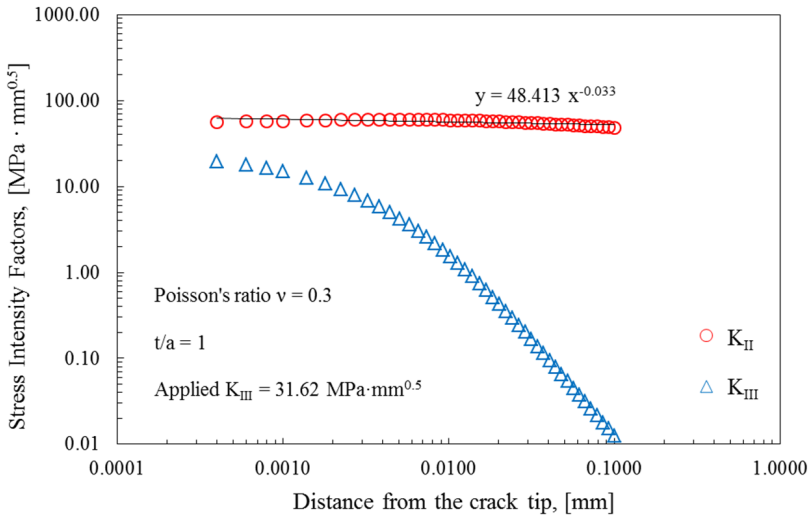

Figure 4: Discs case: K_{II} and K_{III} at s = 0 mm from disc surface, t/a = 1.

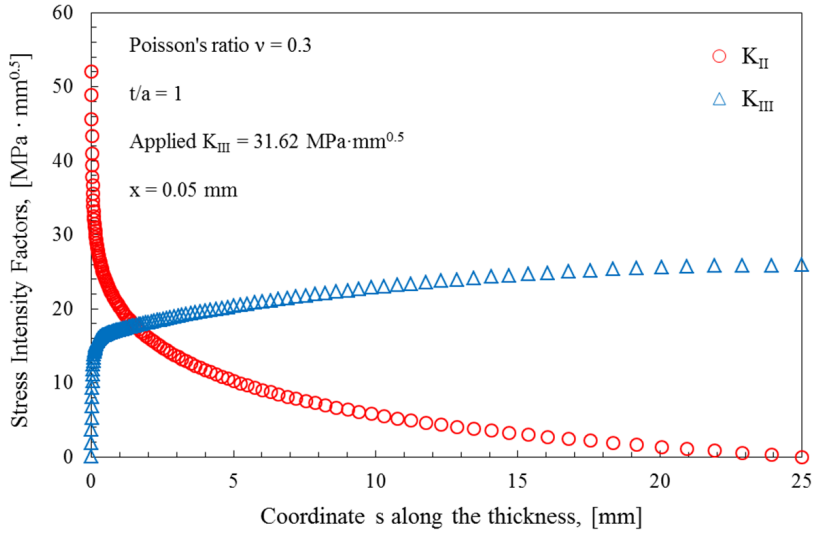

Figure 5: Discs case: through thickness distribution of K_{II} and K_{III} for: $t/a = 1$, $x = 0.05$ mm.

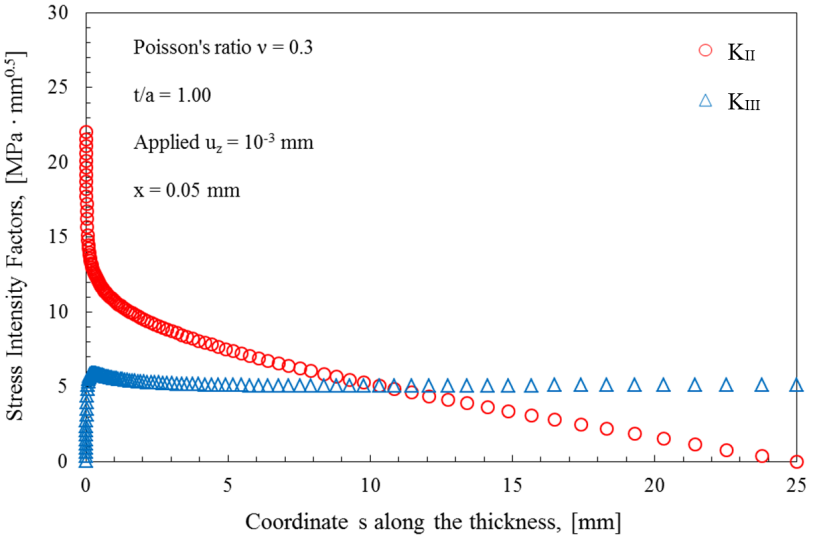

Figure 6: Plates case: through thickness distribution of K_{II} and K_{III} for: $t/a = 1$, $x = 0.05$ mm.

Through-the-thickness distributions of K_{II} and K_{III} for $t/a = 1$ are shown in Figs. 5-6. From Tabs. 1 and 2 the values of K_{II} are not realistic for $s < 0.25$ mm and the values of K_{III} are not realistic for $s < 1$ mm.

For the discs results (Fig. 5) maximum values of K_{III} are at the centreline. The influence of plate bending means that maxima steadily decrease as t/a decreases. Maximum values of K_{III} tend to zero as t/a tends to zero. This is to be expected because K_{III} is not possible in two dimensions. For the thicker discs K_{III} is nearly constant for $s > 50$ mm [2], and then decreases steadily towards the surface, with an abrupt drop close to the surface. For thinner discs behaviour is similar except that there is no constant K_{III} region [2]. Hence, there is clear evidence of an end effect.

For the plates results (Fig. 6) the distributions of K_{III} are significantly different from those for discs results. There are maxima at the centre line but K_{III} then remains nearly constant for about half the distance to the plate surface. The influence of plate bending again means that maxima steadily decrease as t/a decreases. As a surface is approached K_{III} first decreases slightly then increases to a maximum at about 0.15 mm from the surface. There is then an abrupt drop which is within the region where realistic values of K_{III} cannot be calculated.

Plate bending theory [1] suggests that K_{II} should be zero on the centre line, with a linear increase towards a surface. K_{II} does indeed increase linearly for much of the thickness with a greater increase as the surface is approached. This is within

the region where realistic values of K_{II} cannot be calculated. The extent of the linear portion, in terms of plate thickness, decreases as t/a increases but is still present when t/a = 3 [3]. This is in contrast with the discs results [2] where linear portions are less extensive and K_{II} becomes essentially zero for s > 40 mm. Maximum values of K_{II} are at the surface. This is within the region where calculated K_{II} values are not realistic so caution is needed in the interpretation of results.

DISCUSSION

There has been a lot of discussion on whether K_{III} tends to zero or infinity as a corner point is approached [2,3]. When apparent K_{III} values are calculated from stresses at a constant distance from the crack tip then K_{III} appears to tend to zero as the model surface is approached (Fig. 5-6), in accordance with the linear elastic prediction. However, apparent values of K_{III} at the surface (Fig. 4) increase strongly as the distance from the crack tip at which they are calculated decreases. These results can be interpreted as indicating that K_{III} tends to infinity at a corner point in accordance with Bažant and Estenssoro's prediction. The results in Figs. 5-6 also show that K_{II} does appear to tend to infinity as the surface is approached, in accordance with Bažant and Estenssoro's prediction. The discussion is futile because, as pointed out by Benthem [9], K_{III} is meaningless at a corner point and there is no paradox.
For $s \geq 0.25$ mm the value of λ calculated from τ_{xy} is close to the theoretical value of 0.5 for a stress intensity factor singularity so K_{II} provides a reasonable description of the crack tip stress field. Similarly, K_{III} provides a reasonable description of the crack tip stress field for $s \geq 1$ mm. At the surface, values of λ obtained from τ_{xy} are always less than the theoretical value for a corner point singularity. The distribution of τ_{yz} at the surface (Fig. 2) cannot be accounted for on the basis of Bažant and Estenssoro's analysis. There is clear evidence of a boundary layer effect whose extent is independent of the thickness. The only available characteristic dimension controlling the boundary layer thickness is the crack length, a.

STRAIN ENERGY DENSITY THROUGH THE DISC AND PLATE THICKNESS

The intensity of the local stress and strain state through the disc and plate thickness can be easily evaluated by using the strain energy density (SED) averaged over a control volume embracing the crack tip (see Ref. [13] for a review of the SED approach). The main advantage with respect to the local stress-based parameters is that it does not need very refined meshes in the close neighbourhood of the stress singularity [19]. Furthermore the SED has been considered as a parameter able to control fracture and fatigue in some previous contributions [14-18, 22] and can easily take into account also coupled three-dimensional effects [2, 3, 23, 24].
With the aim to provide some numerical assessment of the contribution of the three-dimensional effects, specifically the coupled fracture mode, K_{II}, the local energy density through the disc and plate thickness has been evaluated and discussed in this section.

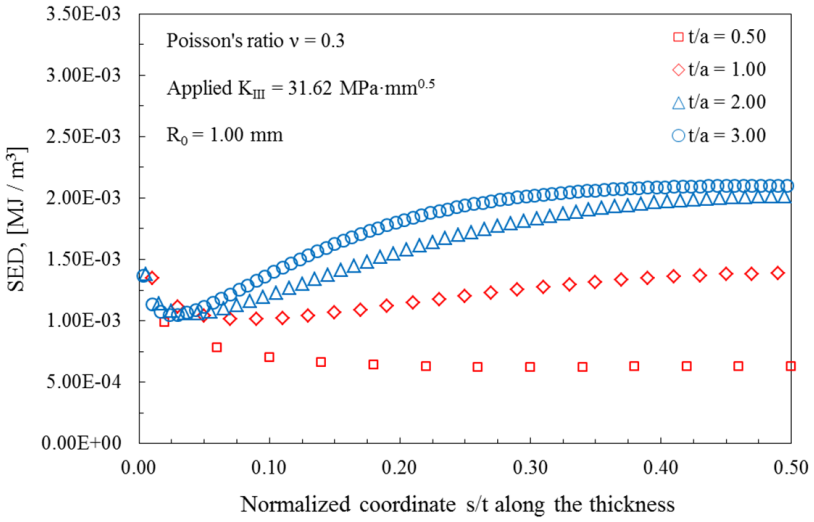

Figure 7: Discs case: through the thickness *SED* distribution for t/a = 0.50, 1, 2, 3. Control radius R_0 = 1.00 mm.

Figs. 7-8 show the local SED variation respectively across the disc and the plate averaged over a cylindrical volume having radius R_0 and height h, with h about equal to R_0. In Refs [13, 14-16, 17-18] R_0 was thought of as a material property which varies under static and fatigue loading but here, for the sake of simplicity, R_0 and h are simply set equal to 1.0 mm, only to quantify the three-dimensional effects through the disc and plate thickness.
The influence of the applied mode III loading combined with the induced singular mode II loading is shown in Figs. 7-8. For the discs results the ratio between the maximum values of K_{II} and K_{III} is quite low (about 2) as can be seen from Fig. 5, so that the maximum contributions are not significantly different and the position of the maximum SED results to be a function of disc thickness [2]. For thin discs it is close to the lateral surface, but for thick discs the maximum SED is at the mid-plane and its value is about 1.5 times the value at the lateral surface.
For the plate results (Fig. 6), indeed, the maximum contribution of the coupled mode II is significantly higher (about 4 times) compared to the maximum contribution of the applied mode III. It is evident that the position of the maximum SED is the same in all cases. It is close to the lateral surface, where the maximum intensity of the coupled mode II takes place, both for thin plates, t/a = 0.5 and 1.0, and for thick ones, t/a = 2 and 3.

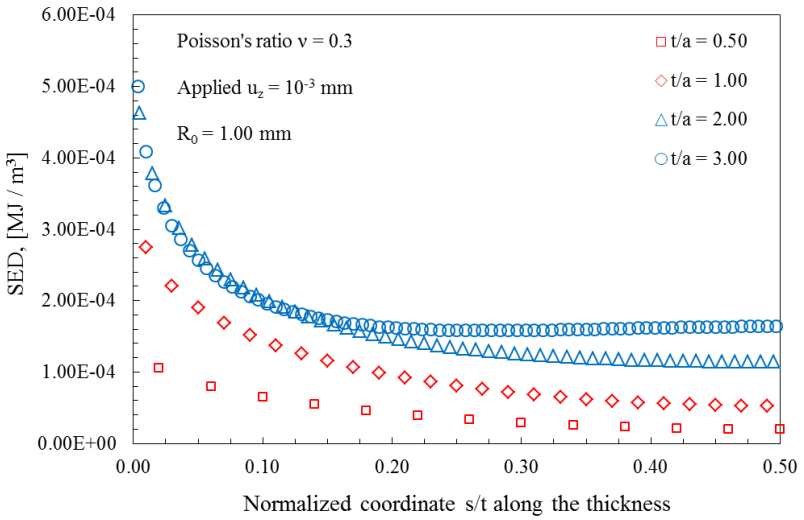

Figure 8: Plates case: through the thickness *SED* distribution for t/a = 0.50, 1, 2, 3. Control radius R_0 = 1.00 mm.

CONCLUSIONS

(1) The results obtained from the highly accurate finite element analyses have improved understanding of the behaviour of through cracked discs and plates under anti-plane loading. In particular, it is confirmed that mode III does induce coupled mode II^c.
(2) The influence of plate bending is increasingly important as thickness decreases. The anti-plane loading used is a nominal mode III loading. For thin discs and plates it is a mixed modes III and II loading, in which mode III induces mode II^c and vice versa. At the present state of the art it is not possible to separate the coupled modes from the applied modes.
(3) Bažant and Estenssoro's analysis works well for the symmetric mode (mode I), but it is incomplete for the asymmetric mode (a combination of modes II and III).
(4) Discussion on whether K_{III} tends to zero or infinity as a corner point is approached is futile because, as pointed out by Benthem, K_{III} is meaningless at a corner point.
(5) The present results do not confirm the existence of a corner point singularity dominated region within a K-dominated region. It appears that a new field parameter, probably a singularity, is needed to describe the stresses at the free surfaces.
(6) Calculation of the strain energy density (SED) in a control volume at the crack tip shows that the position of the maximum SED in the discs case is a function of the thickness. In the plates case instead the position of the maximum SED is independent of plate thickness, contrary to discs results.

(7) Under the anti-plane loading used theoretical understanding of the stress field in the vicinity of a corner point is still incomplete.

REFERENCES

[1] Kotousov, A., Lazzarin, P., Berto, F., Pook, L. P., Three-dimensional stress states at crack tip induced by shear and anti-plane loading, Eng. Fract. Mech., 108 (2013) 65-74. DOI:10.1016/j.engfracmech.2013.04.010.

[2] Pook, L. P., Berto, F., Campagnolo, A., Lazzarin, P., Coupled fracture mode of a cracked disc under anti-plane loading, Eng. Fract. Mech., 128 (2014) 22-36. DOI:10.1016/j.engfracmech.2014.07.001.

[3] Pook, L. P., Campagnolo, A., Berto, F., Lazzarin, P., Coupled fracture mode of a cracked plate under anti-plane loading, Eng. Fract. Mech., (2015). DOI:10.1016/j.engfracmech.2014.12.021.

[4] Pook, L. P., A 50-year retrospective review of three-dimensional effects at cracks and sharp notches, Fatigue Fract. Engng. Mater. Struct., 36 (2013) 699-723. DOI: 10.1111/ffe.12074.

[5] Bažant, Z. P., Estenssoro, L. F., Surface singularity and crack propagation, Int. J. Solids Struct., 15 (1979) 405-426.

[6] Pook, L. P., Some implications of corner point singularities, Eng. Fract. Mech., 48 (1994) 367-378.

[7] Pook, L. P., Linear elastic fracture mechanics for engineers. Theory and applications, WIT Press, Southampton (UK), (2000).

[8] Williams, M. L., On the stress distribution at the base of a stationary crack, J. appl. Mech., 24 (1957) 109-114.

[9] Benthem, J. P., The quarter-infinite crack in a half-space; alternative and additional solutions, Int. J. Solids Struct., 16(2) (1980) 119-130. DOI:10.1016/0020-7683(80)90029-3.

[10] Dhondt, G., On corner point singularities along a quarter circular crack subject to shear loading, Int. J. Fract., 89 (1998) L13-L18.

[11] Paris, P. C., Sih, G. C., Stress analysis of cracks, in: Fracture toughness testing and its applications, ASTM STP 381, American Society for Testing and Materials, Philadelphia (USA), (1965) 30-81.

[12] Timoshenko, S. P., Goodier, J. N., Theory of elasticity, third ed., McGraw-Hill Book Company, New York (USA), (1970).

[13] Berto, F., Lazzarin, P., Recent developments in brittle and quasi-brittle failure assessment of engineering materials by means of local approaches, Mater. Sci. Eng. R, 75 (2014) 1-48. DOI:10.1016/j.mser.2013.11.001.

[14] Lazzarin, P., Berto, F., Elices, M., Gómez, J., Brittle failures from U- and V-notches in mode I and mixed, I+II, mode. A synthesis based on the strain energy density averaged on finite size volumes, Fatigue Fract. Engng Mater. Struct., 32 (2009) 671–684. DOI: 10.1111/j.1460-2695.2009.01373.x

[15] Torabi, A. R., Campagnolo, A., Berto, F., Mode II brittle fracture assessment of key-hole notches by means of the local energy, J. Test. Eval., 44 (2016). DOI: 10.1520/JTE20140295.

[16] Torabi, A. R., Campagnolo, A., Berto, F., Local strain energy density to predict mode II brittle fracture in Brazilian disk specimens weakened by V-notches with end holes, Mater. Design, 69 (2015) 22-29. DOI:10.1016/j.matdes.2014.12.037.

[17] Berto, F., Lazzarin, P., Yates, J. R., Multiaxial fatigue of V-notched steel specimens: A non-conventional application of the local energy method, Fatigue Fract. Engng. Mater. Struct., 34 (2011) 921-943. DOI: 10.1111/j.1460-2695.2011.01585.x.

[18] Berto, F., Campagnolo, A., Lazzarin, P., Fatigue strength of severely notched specimens made of Ti-6Al-4Vunder multiaxial loading, Fatigue Fract. Engng. Mater. Struct., (2015). DOI: 10.1111/ffe.12272.

[19] Lazzarin, P., Berto, F., Zappalorto, M., Rapid calculations of notch stress intensity factors based on averaged strain energy density from coarse meshes: Theoretical bases and applications, Int. J. Fatigue, 32 (2010) 1559-1567.

[20] Yosibash, Z., Shannon, S., Computing edge stress intensity functions (ESIFs) along circular 3-D edges, Eng. Fract. Mech., 117 (2014) 127-151. DOI:10.1016/j.engfracmech.2014.01.013.

[21] Omer, N., Yosibash, Z., On the path independency of the point-wise J integral in three dimensions, Int. J. Fracture, 136 (2005) 1-36. DOI: 10.1007/s10704-005-3934-7.

[22] Torabi, A. R., Campagnolo, A., Berto, F., Experimental and theoretical investigation of brittle fracture in key-hole notches under mixed mode I/II loading, Acta Mech., 226 (2015) 2313-2322. DOI: 10.1007/s00707-015-1323-5.

[23] Campagnolo, A., Berto, F., Lazzarin, P., The effects of different boundary conditions on three-dimensional cracked discs under anti-plane loading, Eur. J. Mech. – A/Solids, 50 (2015) 76-86. DOI:10.1016/j.euromechsol.2014.11.001.

[24] Marangon, C., Campagnolo, A. Berto, F., Three-dimensional effects at the tip of rounded notches subjected to mode-I loading under cyclic plasticity, J. Strain Anal. Eng., 50 (2015) 299-313. DOI: 10.1177/0309324715581964.